Launch Environment Water Flow Simulations Using Smoothed Particle Hydrodynamics

Bruce T. Vu* Jared J. Berg† Michael F. Harris†
NASA Kennedy Space Center, FL 32899, USA

Alejandro C. Crespo‡
Universidade de Vigo, Spain

This paper describes the use of Smoothed Particle Hydrodynamics (SPH) to simulate the water flow from the rainbird nozzle system used in the sound suppression system during pad abort and nominal launch. The simulations help determine if water from rainbird nozzles will impinge on the rocket nozzles and other sensitive ground support elements.

I. Introduction

One of the crucial ground structures employed at the launch pad is the rainbird nozzle system, whose primary objective is to suppress acoustic energy generated by the launch vehicle during pad abort and nominal operations. It is important that the rainbird water flow does not impinge on the rocket nozzles and other sensitive ground support elements. Figure 1 shows the rainbird system employed during the Space Shuttle program. These rainbirds were located on the North deck of the mobile launcher platform and were activated at T-0, so they didn't really pose a threat to the launch vehicle. For the new Space Launch System (SLS) vehicle the operation is similar, regardless of the new mobile launcher and new engine configurations. The goal of the rainbird nozzle system remains the same, which is sound suppression (SS), and the rocket engines still cannot get wet. However, the rearrangement of the rainbird water system for the SLS mobile launcher, as shown in Figure 2, locates the rainbirds closer to the first-stage rocket engines, which are positioned above the exhaust hole and not shown in the picture. The close proximity of the rainbird nozzle system could potentially cause vehicle wetting during liftoff.

This paper describes the numerical simulation of water flow using SPH in an attempt to determine if rainbird water would have an impact during abort and launch operations.

II. Modeling

The advantage of Smoothed Particle Hydrodynamics (SPH) is that it is a meshfree, nodal collocation, spatial discretization, kernel approximation method; therefore, the pre-processing step is completely avoided and grid quality is no longer an issue.[1] Like other particle methods, SPH was known for its computationally intensive drawback in problems using fine description. However, with recent advances of hardware acceleration and parallel computing such as Graphical Processing Unit (GPU), SPH technology has become more useful and versatile.

Water is delivered from an elevated water tank to the rainbird nozzle system via gravity.[2] This tower is 90m high and located 200m from the launch deck, resulting in a large computational domain for SPH. Therefore, the alternative is to model a cylindrical tank underneath the rainbird nozzles, below the launch deck, and water will be pushed using a plunger, as shown in Figure 3. The speed of the plunger is calculated to match the volume flow rates through the rainbird nozzle outlets. As long as the water volume flow rates

*Lead, Fluid Systems Group, Senior Member AIAA.
†AST Fluid Mechanics.
‡Main Developer & Research Fellow.

are matched, the actual flow conditions have been simulated. The time-history volumetric profiles for the pad abort and nominal launch are shown in Figures 4 and 5, and the peak flow rates through all the rainbird nozzles are listed in Table 1.

	Rainbird Nozzle System		
Operation	North East/ North West	North Center	South East/ South West
Nominal	72,491	85,148	115,065
Abort	35,783	42,031	56,798

Table 1. Peak Water Flow Rates in GPM

Graphical Processing Units (GPUs) appear as a cheap alternative to handle High Performance Computing for numerical modeling. GPUs are designed to manage huge amounts of data and their computing power has increased in much faster than the Central Processing Units (CPU). Compute Unified Device Architecture (CUDA) is a parallel programming method and software for parallel computing with some extensions to C/C++ language. The parallel power computing of GPUs can also be applied for SPH methods where the same loops for each particle along the simulation can be parallelised.

The simulations are based on DualSPHysics solver, which has been implemented in C++ and CUDA language to carry out simulations on the CPU and GPU, respectively. DualSPHysics is open-source and can be freely downloaded from "ww.dual.sphysics.org". The object-oriented programming paradigm makes the code easy to understand, maintain and modify. A sophisticated control of errors is available. Furthermore, better approaches are implemented, for example particles are reordered to give faster access to memory, symmetry is considered in the force computation to reduce the number of particle interactions and the best approach to create the neighbour list is implemented.[3] The CUDA language manages the parallel execution of threads on the GPUs. The best approaches were considered to be implemented as an extension of the C++ code, so the best optimizations to parallelise particle interaction on GPU were implemented.[4] Preliminary results were presented in Crespo et al[5] and the first rigorous validations were presented in Crespo et al.[6] A complete description of DualSPHysics can be found in Crespo et al.[7]

III. Governing Equations

In order to perform water flow simulations, we need to solve the system of differential equations:

$$\frac{D\rho}{Dt} = -\rho\nabla\cdot\vec{v} \tag{1}$$

$$\frac{D\vec{v}}{Dt} = -\frac{1}{\rho}\nabla p + \nu\nabla^2\vec{v} + \vec{g} \tag{2}$$

which are known as Navier-Stokes equations for Newtonian incompressible flows. In these equations, ρ represents the fluid's density, $\vec{v}$ the velocity field, p the pressure field, $\vec{g}$ the resultant of external forces and ν the fluid's kinematic viscosity. These equations can be rewritten in compact matrix form, for the domain and boundary:

$$A(f(r)) = \nabla\sigma + F, \qquad \forall r \in \Omega \tag{3}$$

$$B(f(r)) = \bar{f}, \qquad \forall r \in \Gamma \tag{4}$$

Let $f^h(r)$ be an approximation of $f(r)$:

$$f(r) \approx f^h(r) = \sum_{i=1}^{n} N_i(r) f_i \tag{5}$$

where $f_i = f(r_i)$ is nodal value of $f(r)$ at specified particle r_i and $N_i(r)$ is the shape function used to interpolate field $f(r)$ from f_i.

For any test function v in the domain Ω and boundary Γ, equations 3 and 4 become:

$$\int_{\Omega} v^T A(f(r))d\Omega + \int_{\Gamma} \bar{v}^T B(f(r))d\Gamma = 0 \tag{6}$$

The test function v can be constructed by some basis function $\bar{\Phi}_i$:

$$v = \sum_{i=1}^{r} a_i \Phi_i \quad \text{and} \quad \bar{v} = \sum_{i=1}^{r} b_i \bar{\Phi}_i \tag{7}$$

leading to the final weighted residual function:

$$\int_{\Omega} \Phi^T A(f(r))d\Omega + \int_{\Gamma} \bar{\Phi}^T B(f(r))d\Gamma = 0 \tag{8}$$

Nodal Collocation

Point collocation discretizes the weighted residual function based on a Dirac delta function

$$\delta(r) = \begin{cases} 0 & r \neq 0 \\ 1 & r = 0 \end{cases} \tag{9}$$

Dirac delta function has some useful properties:

$$\int_{\Omega} \delta(r)dr = 1 \quad \text{and} \quad \int_{\infty}^{\infty} \delta(r = r')f(r')dr' = f(r) \tag{10}$$

For a boundary value problem,

$$A(f(r)) = 0, \qquad \forall r \in \Omega \tag{11}$$

$$B(f(r)) = 0, \qquad \forall r \in \Gamma \tag{12}$$

Using the delta function $\delta(r_i - r)$ as test function, a set of collocation equations can be derived:

$$A(f^h(r_i)) = 0, \qquad i = 1, 2, ..., r_1 \tag{13}$$

$$B(f^h(r_j)) = 0, \qquad j = 1, 2, ..., r_2 \tag{14}$$

where r_1 and r_2 are particles in Ω and Γ, respectively.

Kernel Approximation

In a Kernel approximation, the δ function can be replaced by a smoothing function $w(r - r', h)$ which is an even function and satisfies the following conditions:

$$\int_{\Omega} w(r - r', h)dr' = 1 \qquad \lim_{h \to 0} w(r - r', h) = \delta(r - r') \tag{15}$$

$$w(r - r', h) = 0 \quad \text{for} \quad |(r - r')| > \kappa h \tag{16}$$

where constant κ defines the compact support of smoothing function, and $f(r)$ can be approximated as

$$f^h(r) = \int_{\Omega} f(r')w(r - r', h)dr' \tag{17}$$

The integral form can be discretized by particle approximation:

$$f^h(r) = \sum_{i=1}^{n} w_i(r) \Delta V_i f_i \tag{18}$$

where $w_i(r) = w(r - r_i)$ and ΔV_i is the volume of particle r_i.

In SPH, finite volume of particle is related to mass of particle through density ($m_i = \rho_i \Delta V_i$). The approximate function in Equation 18 can be written as

$$f^h(r) = \sum_{i=1}^{n} w_i(r) \frac{m_i}{\rho_i} f_i \tag{19}$$

The approximate solution of particle i is

$$f^h(r_i) = \sum_{j=1}^{n} w_i j(r) \frac{m_j}{\rho_j} f(r_j) \tag{20}$$

where $w_{ij} = w(r_i - r_j, h)$, thus the density of particle i becomes

$$\rho_i = \sum_{j=1}^{n} w_{ij} m_j \tag{21}$$

The above equation shows that particle density is based on smoothing of the surrounding particle masses, therefore the name "smoothed particle".[1]

IV. Discussion of Results

Several test cases have been performed to check out the flow patterns. Water can be rejected through the nozzle by plunger, of which the motion is described by acceleration, velocity, or position. Figures 6 and 7 show the water flow due to acceleration and velocity of the plunger, respectively. SPH simulations of water flow through an actual rainbird nozzles are performed and compared against predictions obtained from other methods such as 1-D projectile and 2-D Volume of Fluid (VOF) analyses.[8] Figure 8 shows the 1-D projective analysis, for which the South rainbird flow rate is at 56,798 GPM during the abort case. The 2-D VOF simulation in Figure 9 shows the velocity of water flow as well as throw distance for the same rainbird. SPH simulations are made for the North and South rainbirds, respectively, for the low and high flow rates (Figures 10-11). The concentric circles in these figures indicate the throw distance depicted by 1-D projectile analysis. It can be seen that SPH results are bounded, thus in good agreement with the other methods.

Figures 12-13 show the water flow patterns during a nominal launch. The water jets ejected from the rainbirds appear to develop gradually over the exhaust hole prior to T-zero. When water flow is fully developed and completely covers the hole, the launch vehicle already lifts off. There might be some water splashing off the deck and sprinkling on the rockets. However, the impact is minimal and acceptable.

During a pad abort event, it is important that the Hydrogen Burn-Off Igniter (HBOI), shown in Figure 14, is kept dry. The simulations show that the HBOI will get doused in the baseline design (Figure 15), unless there is some blockage to fill the gap between the launch deck and the blast shield, in the vicinity of the HBOI. A triangular wedge has been considered among many design concepts for this blockage. Figure 16 shows the region near the HBOI, with the ML made transparent for visualization purposes. The wedge underneath the blast shield deck is designed to prevent water from deluging the HBOI. This wedge design effectively keeps water from getting to the HBOI, as shown in Figures 17 and 18 for North Center rainbird and Figure 17 for South rainbirds.

Another piece of GSE that cannot get wet during operation is the camera housing located inside the exhaust hole (Figure 20). The simulations show that a strong wave formed between the rainbirds will downpour over the haunch where the camera is installed (Figure 21). Instead of the wedge design, a dam can be built to block the entire gap under the blast shield and over the edge of the exhaust hole (Figure 22). This dam design also effectively prevents the HBOI and other sensitive GSE's from getting wet (Figure 23).

V. Conclusion

The SPH simulation has been used to determine the water flow related to the rainbird water nozzle system. The results can be used to determine if the system can meet the requirement of sound suppression while keeping the SLS rocket engines and other sensitive ground support elements dry during nominal launch and pad abort operations. The water flow rates and timing have a significant impact on vehicle wetting and impingement of launch pad GSE's. In addition to changing the flow rates and timing, the IOP/SS engineers have several design options in case the rainbird water flow could wet rocket engines during launch. These options include rearranging the nozzle system, lowering the rainbird nozzle, or changing its injection angle.

Acknowledgement

The rainbird water nozzle redesign project was supported by the KSC Ground Support and Development Operations (GSDO) office, with Mr. Eric Ernst as the Mobile Launcher program manager.

References

[1]G.R. Liu, "Smoothed Particle Hydrodynamics: A Meshfree Particle Method," World Scientific, ISBN-13: 978-9812384560.

[2]Vu, B. T., Berg, J. J., and Harris, M. F., "Launch Environment Water Flow Simulation Using Smoothed Particle Hydrodynamics (SPH)," Applied Modeling and Simulation (AMS) seminar, NASA Ames Research Center, 18 April 2014.

[3]Dominguez JM, Crespo AJC, Gómez-Gesteira M and Marongiu JC (2010) Neighbour lists in Smoothed Particle Hydrodynamics. International Journal for Numerical Methods in Fluids. doi: 10.1002/fld.2481.

[4]Crespo AJC, Marongiu JC, Parkinson E, Gómez-Gesteira M, Dominguez JM (2009) High Performance of SPH Codes: Best approaches for efficient parallelization on GPU computing. Proc IVth Int SPHERIC Workshop (Nantes), 69-76.

[5]Crespo AJC, Dominguez JM, Barreiro A and Gómez-Gesteira M (2010) Development of a Dual CPU-GPU SPH model. Proc 5th Int SPHERIC Workshop (Manchester), 401-407.

[6]Crespo AJC, Dominguez JM, Barreiro A, Gómez-Gesteira M and Rogers BD (2011). GPUs, a new tool of acceleration in CFD: Efficiency and reliability on Smoothed Particle Hydrodynamics methods. PLoS ONE. doi:10.1371/journal.pone.0020685.

[7]Crespo AJC, Domínguez JM, Rogers BD, Gómez-Gesteira M, Longshaw S, Canelas R, Vacondio R, Barreiro A, García-Feal O (2014). DualSPHysics: open-source parallel CFD solver on Smoothed Particle Hydrodynamics (SPH). Computer Physics Communications. doi: 10.1016/j.cpc.2014.10.004.

[8]Vu, B. T., Moss, N. R., and Sampson, Z., "Multi-Phase Modeling of Rainbird Water Injection," AIAA Aviation and Aeronautics Forum and Exposition, June 16-20, 2014, Atlanta, GA.

Figure 1. Shuttle Rainbirds.

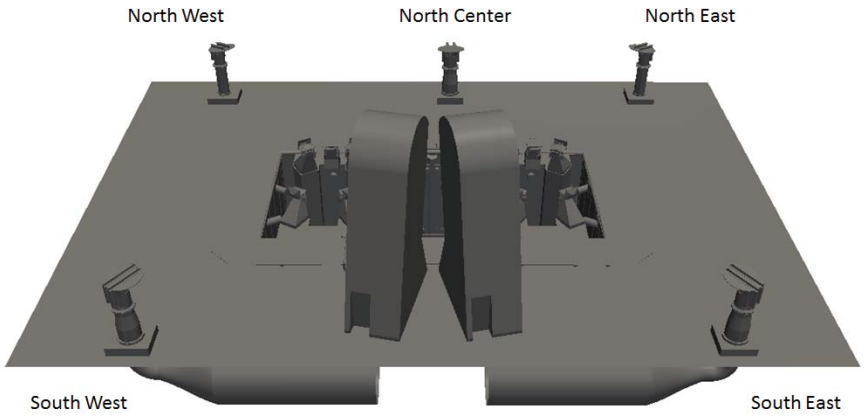

Figure 2. SLS Rainbird Nozzle System.

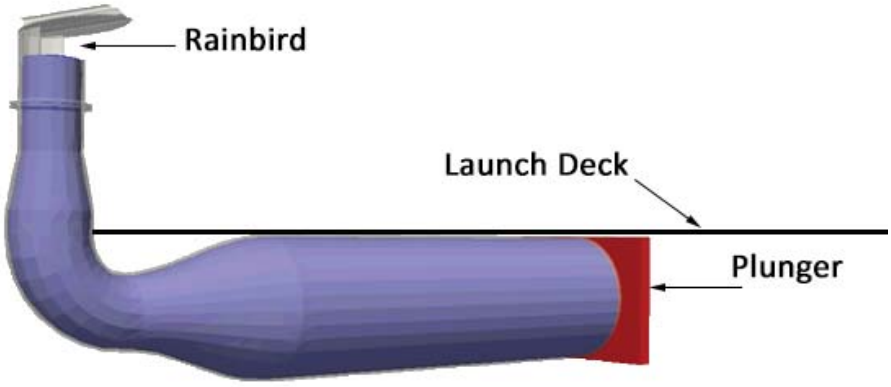

Figure 3. Water Tank Setup.

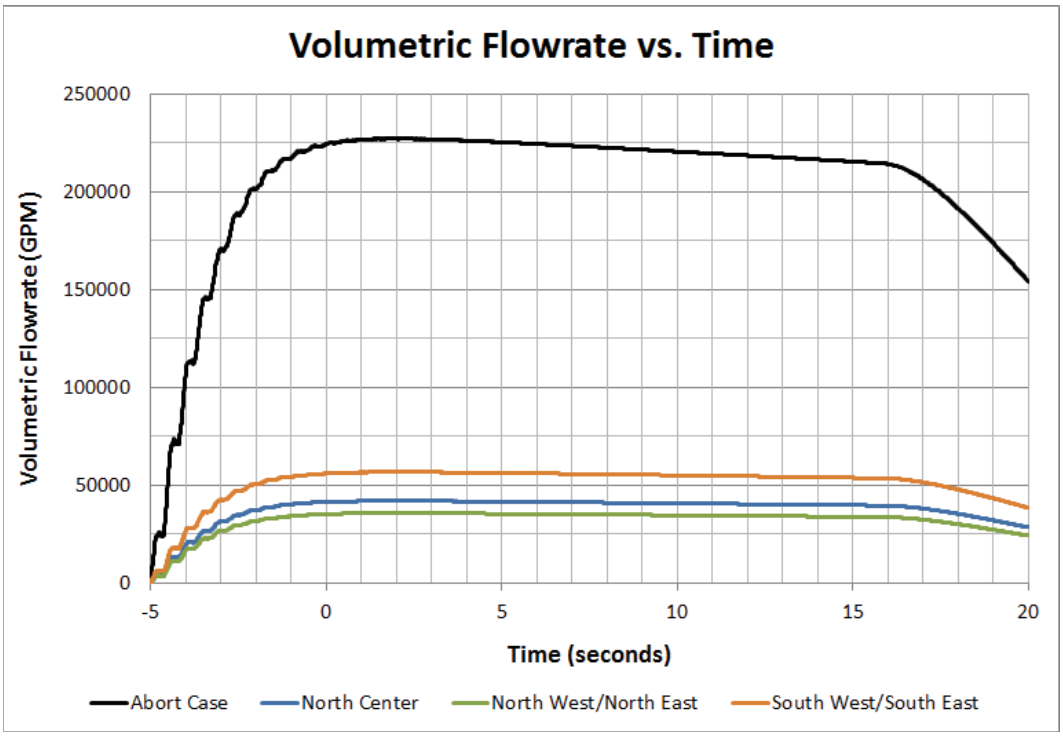

Figure 4. Pad Abort Water Flow.

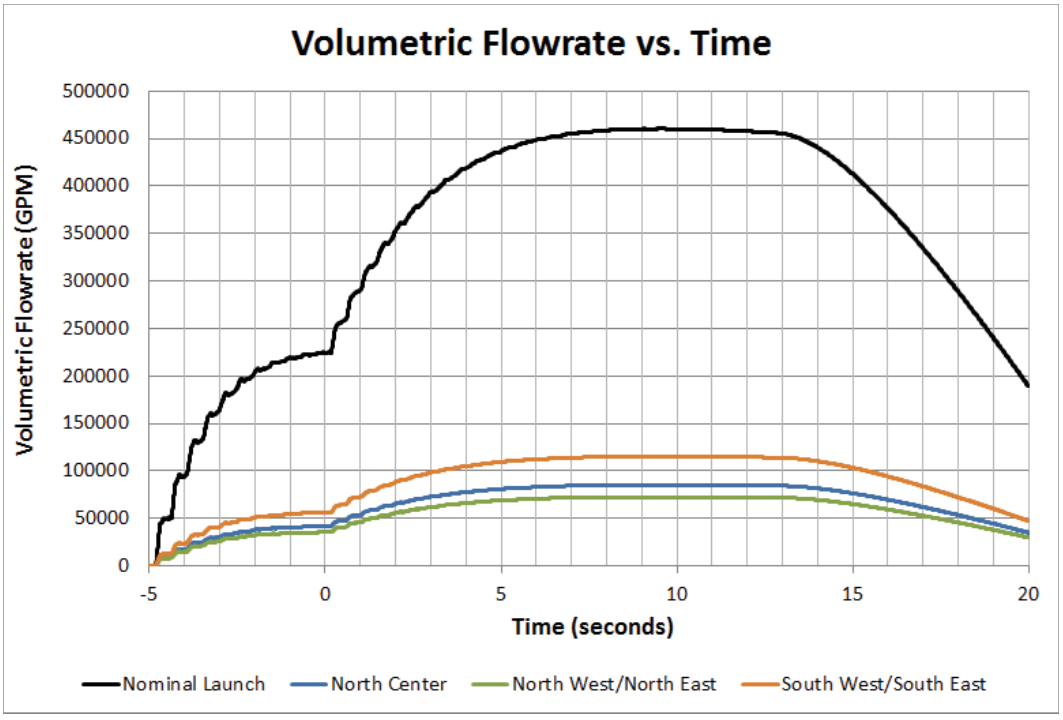

Figure 5. Nominal Launch Water Flow.

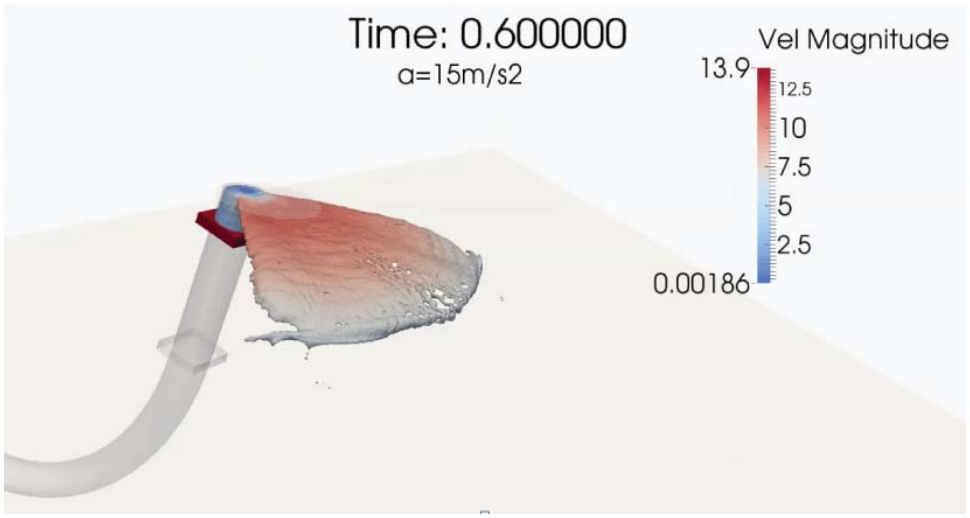

Figure 6. Test Case 1 - Acceleration.

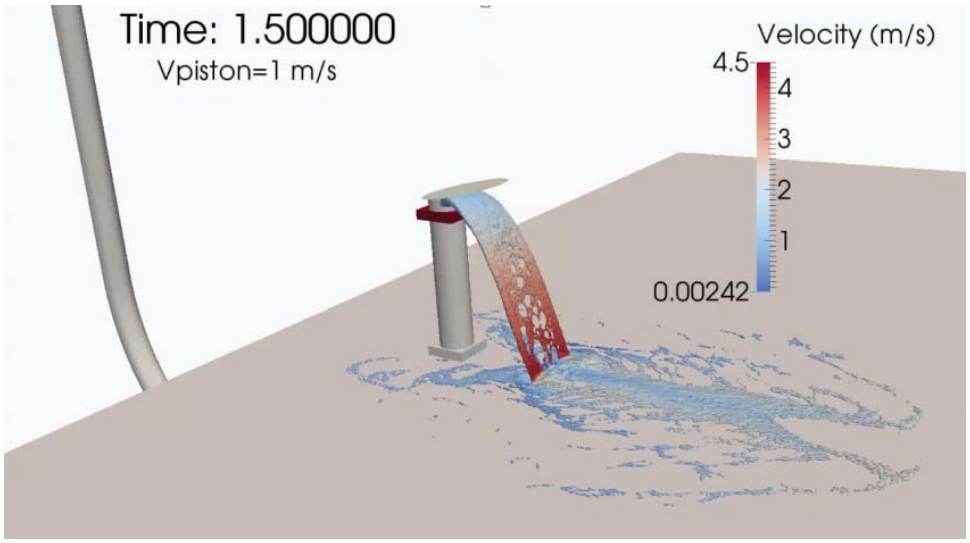

Figure 7. Test Case 2 - Velocity.

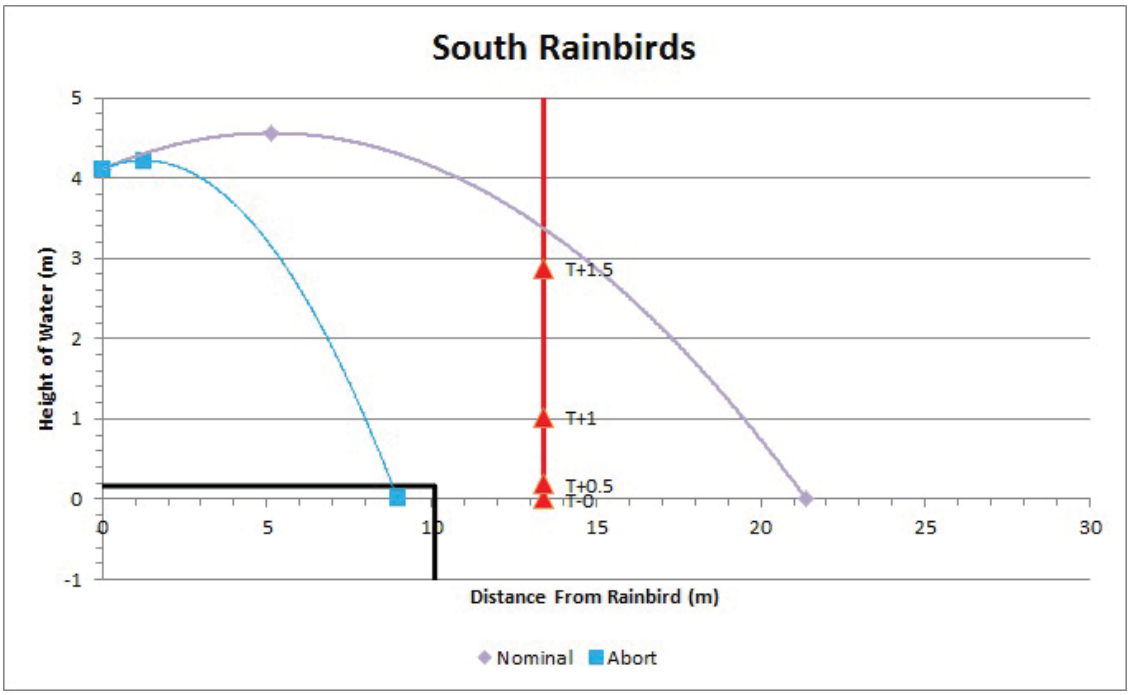

Figure 8. 1-D Projectile Prediction (South).

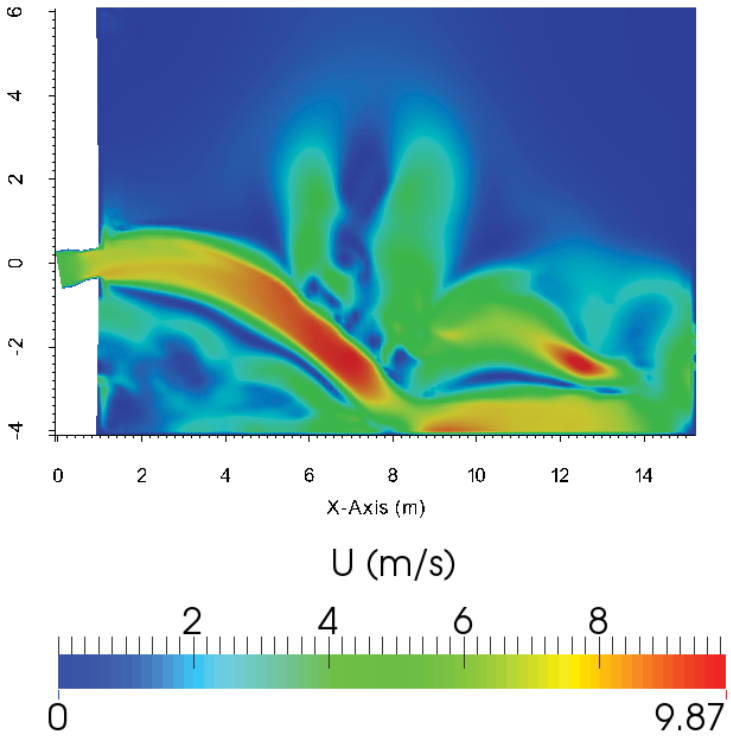

Figure 9. Velocity Magnitude for South Rainbird (Abort - 56,798 GPM).

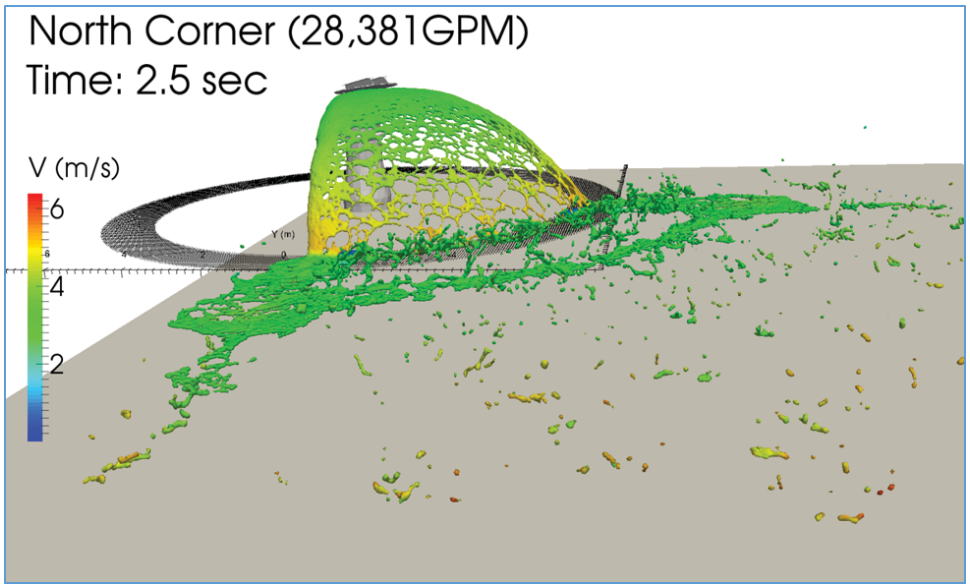

Figure 10. Test Case 3 - Low Flow.

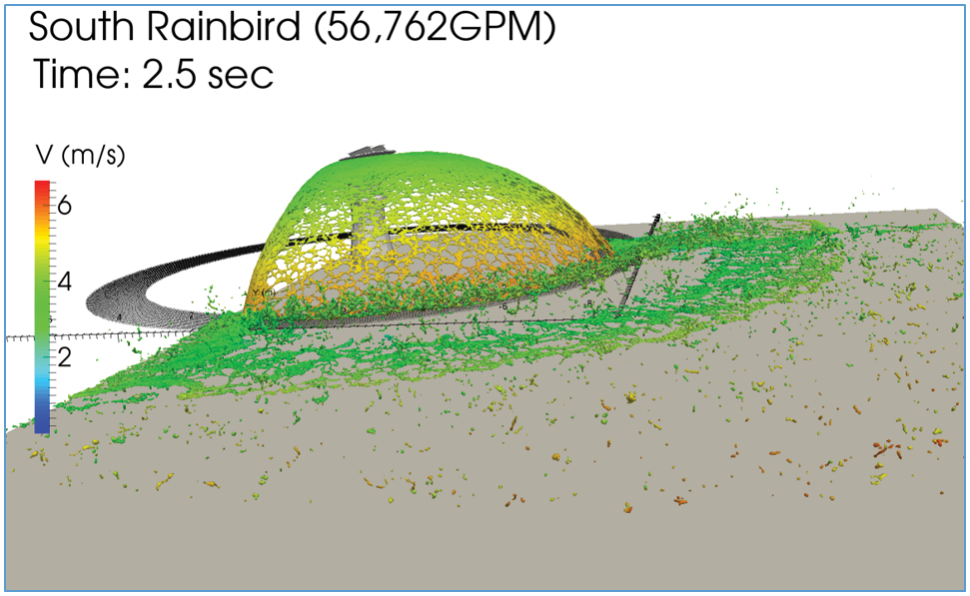

Figure 11. Test Case 4 - High Flow.

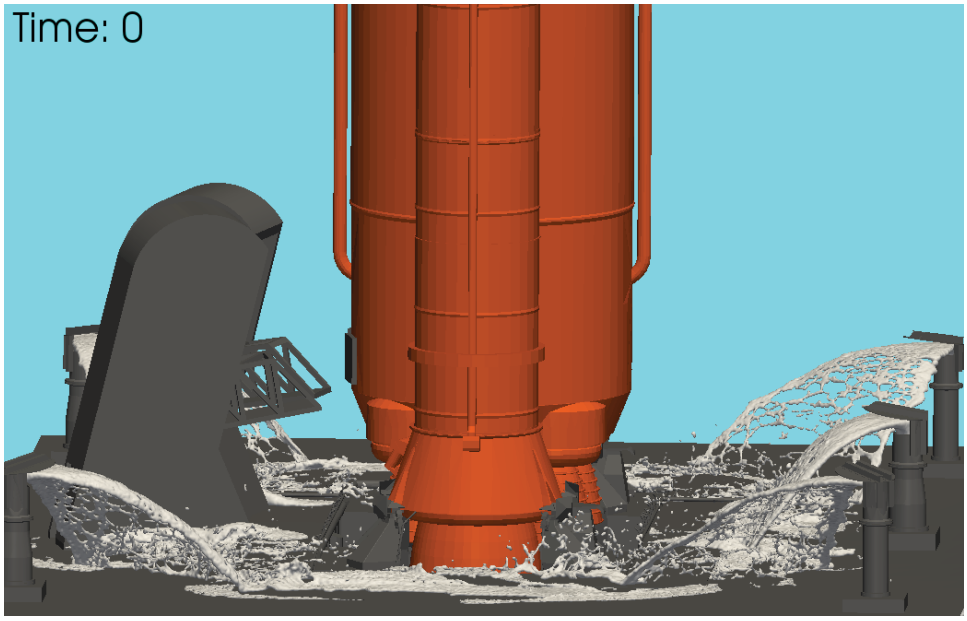

Figure 12. Nominal Launch - T-zero.

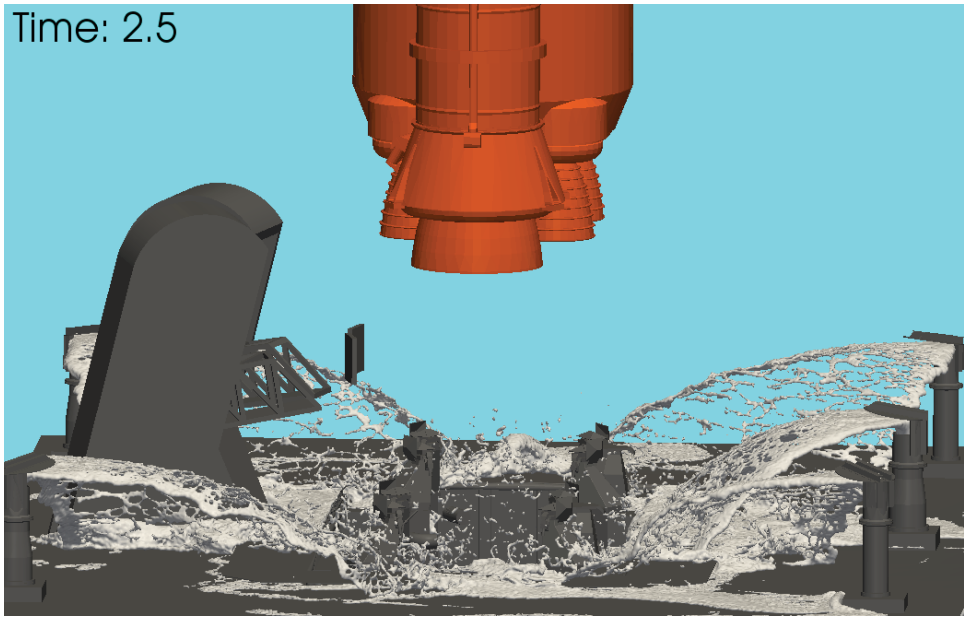

Figure 13. Nominal Launch - T+2.5s.

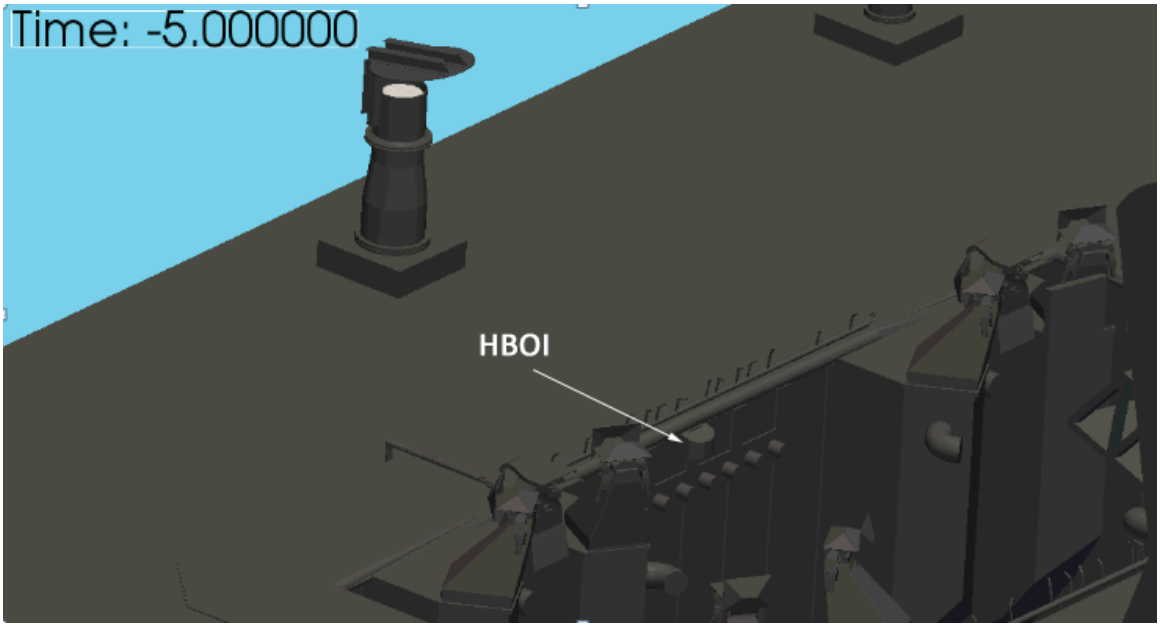

Figure 14. Hydrogen Burn-Off Igniter.

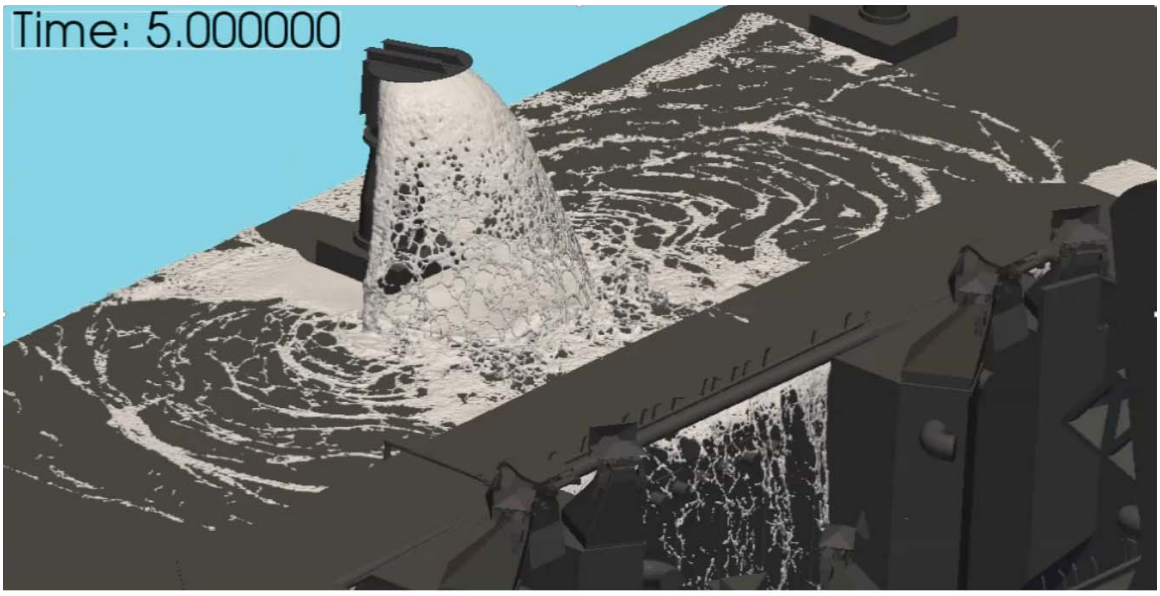

Figure 15. Baseline Design.

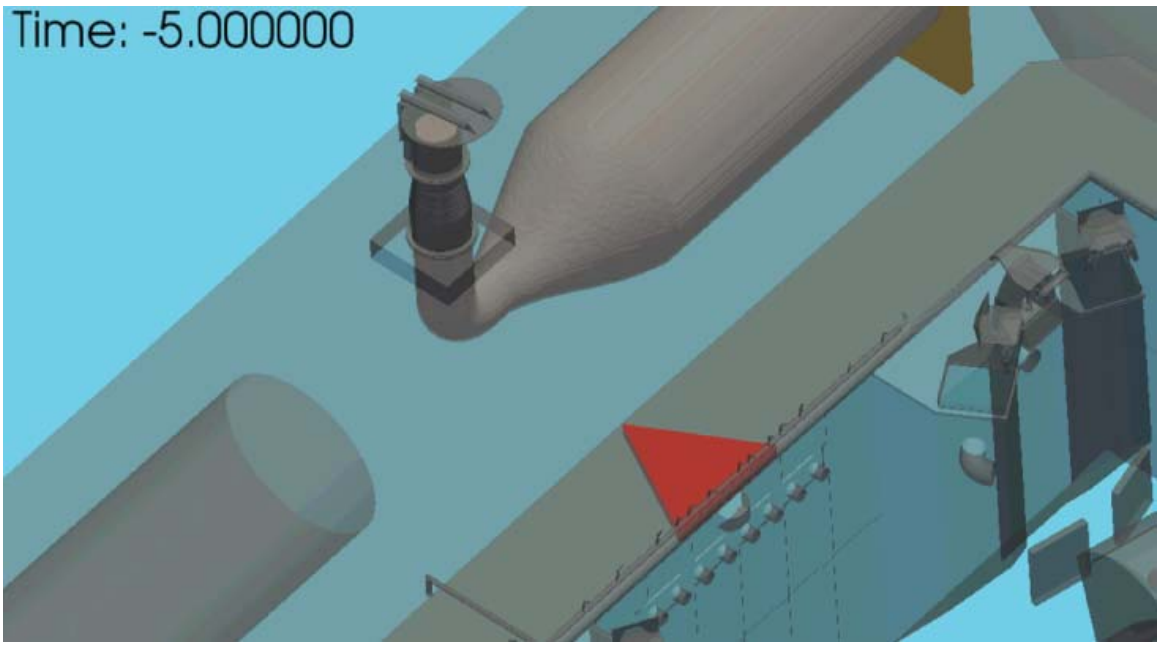

Figure 16. Wedge Design.

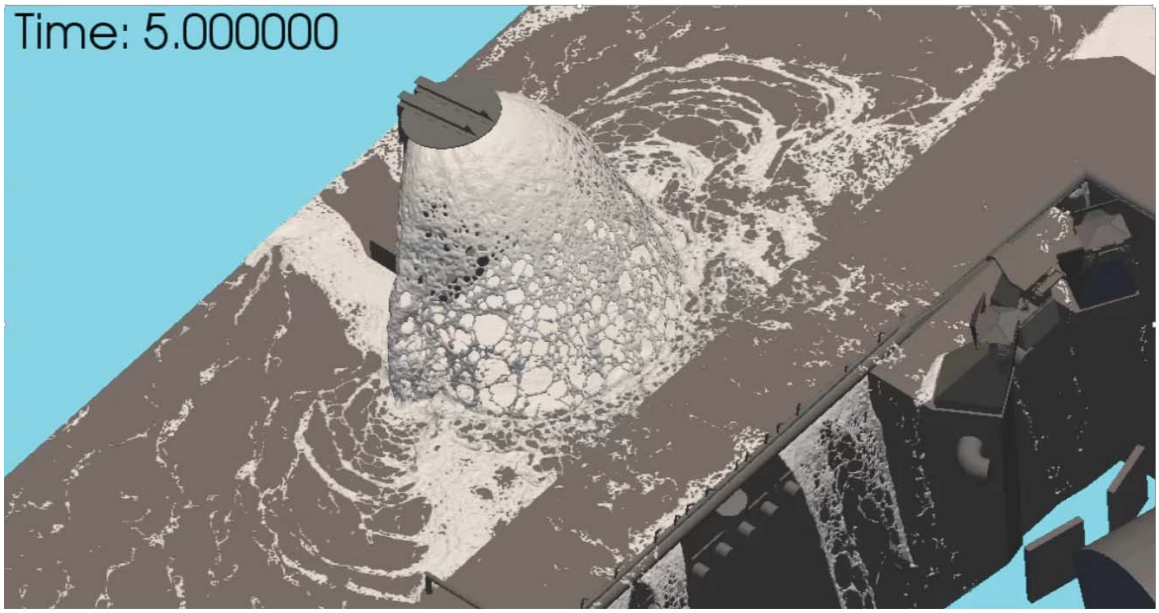

Figure 17. Water Flow with Wedge

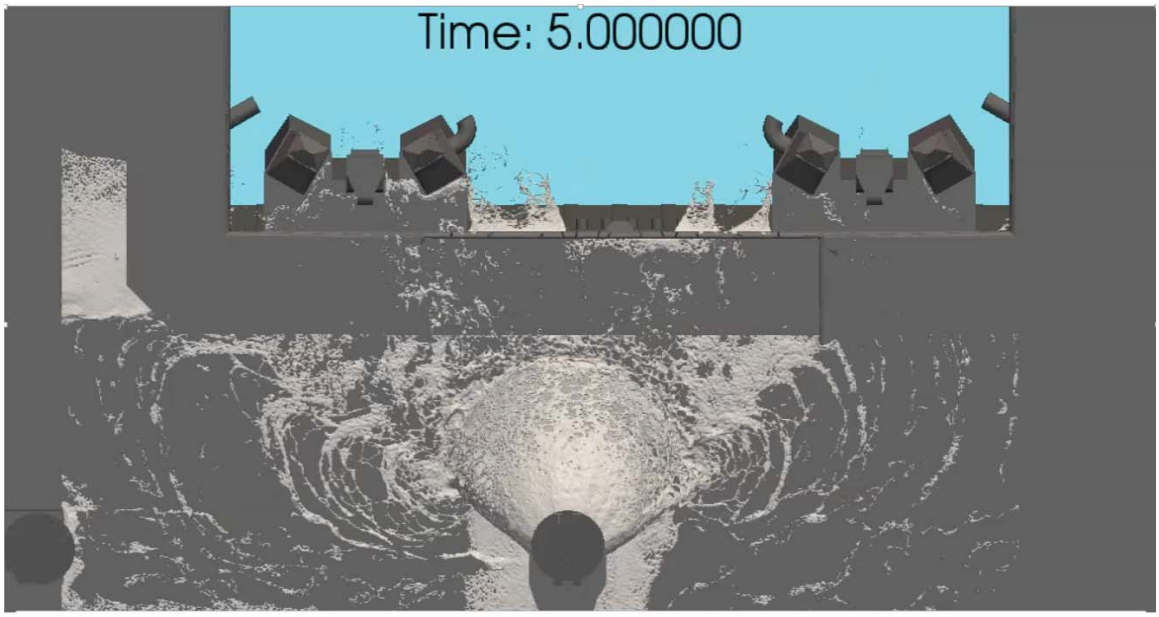

Figure 18. North Center Rainbird Water Flow with Wedge.

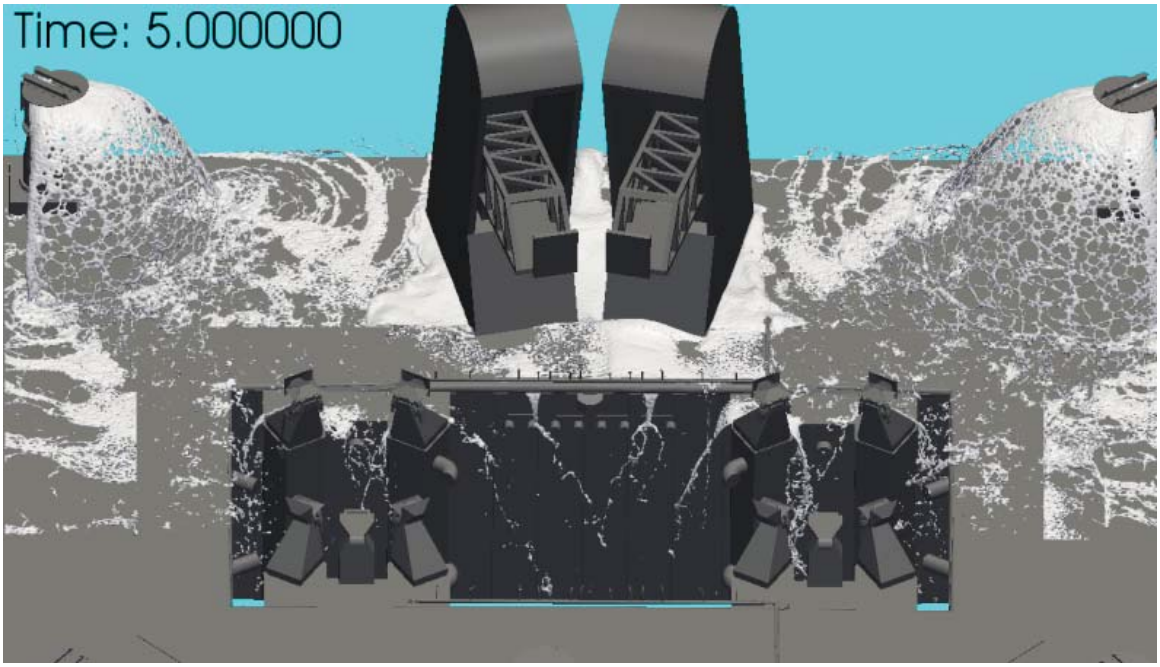

Figure 19. South Rainbird Water Flow with Wedge

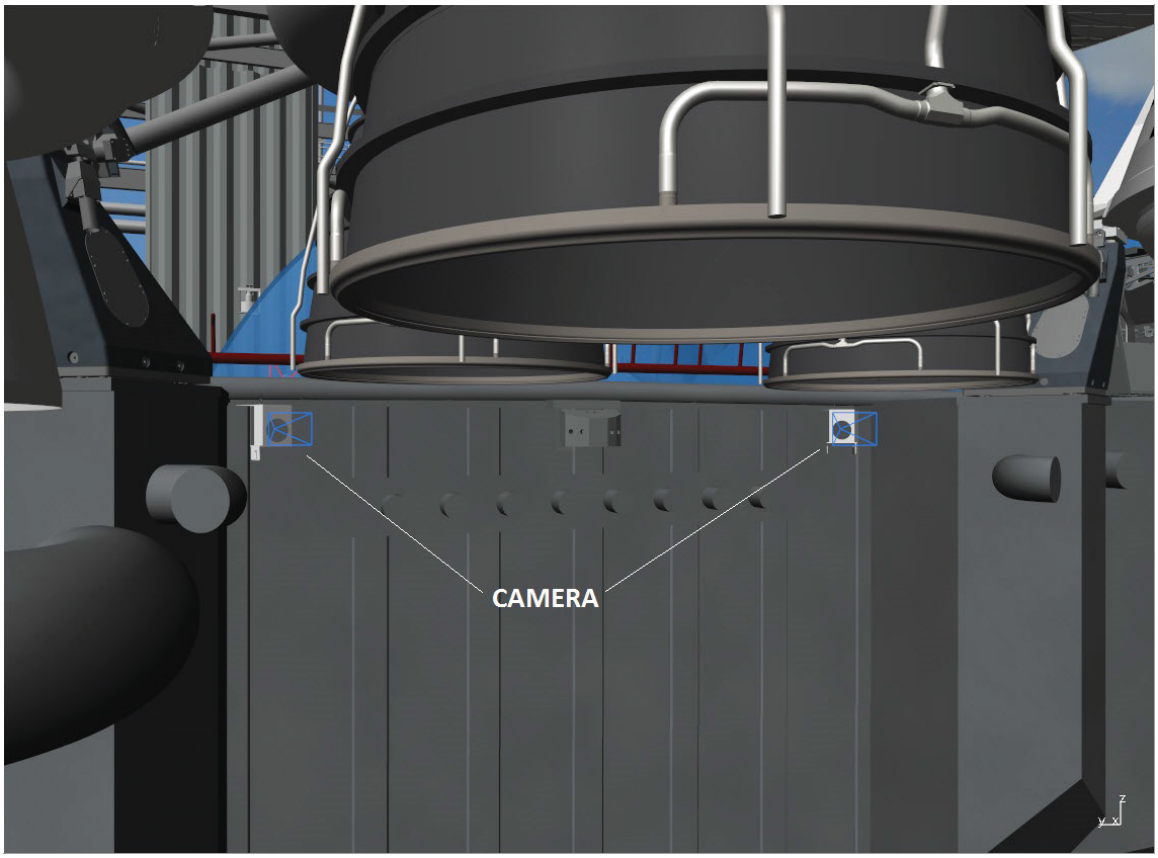

Figure 20. Camera Housing.

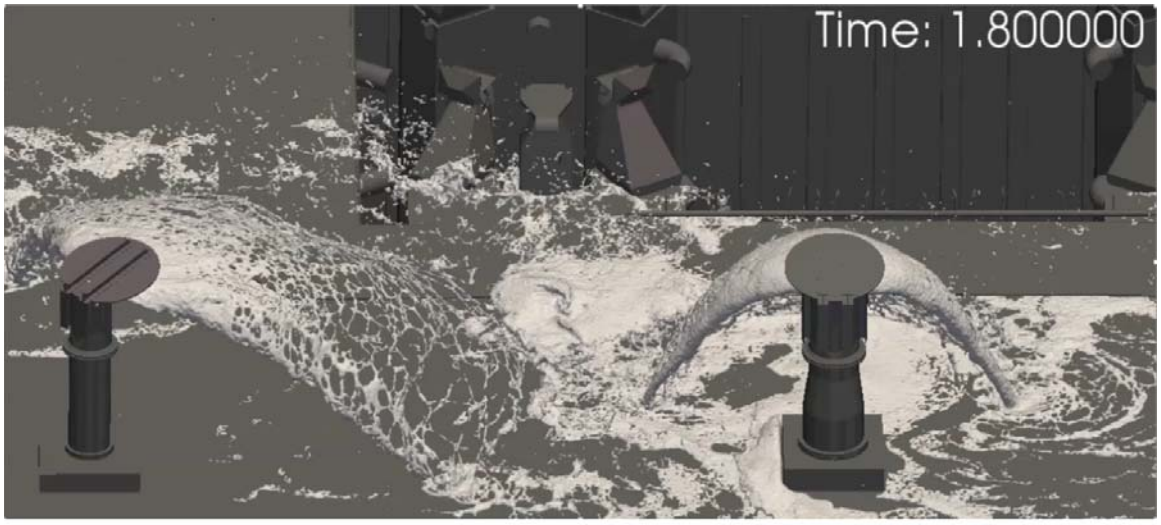

Figure 21. Water Flow over Haunch

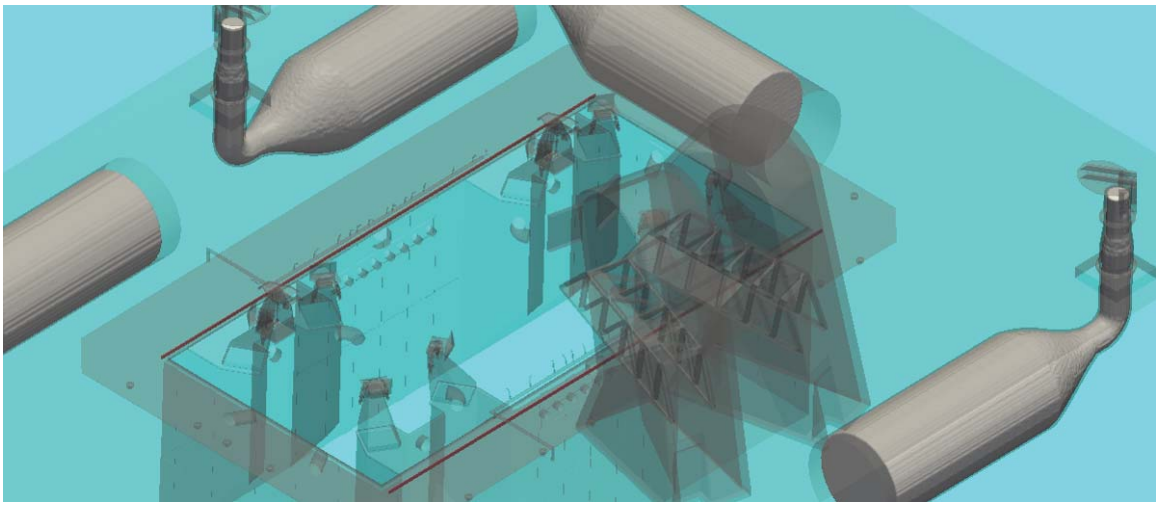

Figure 22. Dam Design.

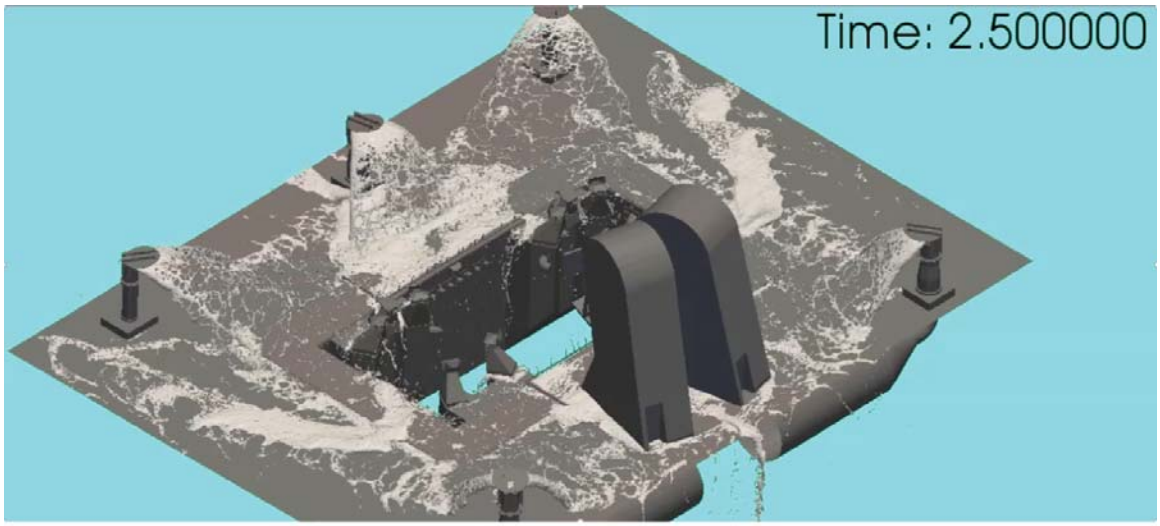

Figure 23. Water Flow with Dam